Available online at www.sciencedirect.com

ScienceDirect

Procedia CIRP 62 (2017) 487 – 493

www.elsevier.com/locate/procedia

10th CIRP Conference on Intelligent Computation in Manufacturing Engineering - CIRP ICME '16

A comparison between 3D Printing and Milling process for a Spar Cap Fitting (wing-fuselage) of UAV Aircraft

Carlo Giovanni Ferro[a]*, Andrea Mazza[a], Dario Belmonte[a], Carlo Seclì[b], Paolo Maggiore[a]

[a]*Politecnico di Torino, Corso Duca degli Abbruzzi 24, Torino 10129, Italy*
[b]*Altair Engineering srl, Via Livorno 60 c/o Environment Park, Torino 10144, Italy*

* Corresponding author. Tel.: +39.011.090.6858;. E-mail address: carlo.ferro@polito.it,

Abstract

Topology optimization is playing an important role in the aircraft design. The demand of lower fuel consumption reflects on the optimization of the airframe of flying vehicles to reduce the structure weight, therefore improving the fraction of the payload. This work focuses on the replacement of an existing part (spar cap fitting) with the new topologically optimized part to be manufactured with 3D printing (Selective Laser Sintering -SLS). The manufacturing constraints (minimum dimension, growth orientation) influence on the optimal results is evaluated to compare traditional milling process' performance with the new SLS technique.

Peer-review under responsibility of the scientific committee of the 10th CIRP Conference on Intelligent Computation in Manufacturing Engineering

Keywords: Topology Optimization; 3Dprinting; Selective Laser Sintering; Structural Optimization.

Nomenclature

DMLS Direct Metal Laser Sintering
EBM Electron Beam Melting
GMAW Gas Metal Arc Welding
MALE Medium Altitude Long endurance
MTOW Maximum Take Odd Weight
SLM Selective Laser Melting
SLS Selective Laser Sintering
SPC Single Point Constraint
UAV Unmanned Aerial Vehicle

1. Introduction

Modern aviation is going towards unmanned vehicles. Starting from Military Aircraft Hale and Male (respectively High and Medium Altitude Aircraft) the Manufacturers are designing and building new flying models that should replace some current manned vehicles in the so-called 3D applications (Dangerous Dirty and Dull) (1) also in civil applications. This aircraft is gaining market share due to different reasons: a) they are more expendables compared to a manned aircraft thanks to the absence of the pilot; b) UAV are simpler and stiffener due to the absence of the life-supporting on-board system (pressurization, temperature control etc.); c) they are cheaper. According to the last point Austin (1) argues that a UAV is smaller, has less operative, fuel and hangarage costs compared to a manned vehicle. Moreover, a UAV designed for surveillance can have the 3-4% of the weight of a manned, 25% of the size and 2.5% or the required power (comparison between ATR 42 and Predator B). It follows that the so called first cost can be reduced up to the 3% of the manned aircraft. The operative cost however remains higher, estimated at the 40% of the manned one.

Also for this type of aircraft the reduction of structural masses is of primary importance to improve the payload mass and to reduce the fuel consumption and the gas emissions (2). In this paper a Topology optimization on a Spar Cap Fitting will be presented, illustrating the possible improvements introducing a new manufacturing technology (Additive manufacturing SLS), (3) to replace an existing part manufactured with the traditional milling process.

Peer-review under responsibility of the scientific committee of the 10th CIRP Conference on Intelligent Computation in Manufacturing Engineering
doi:10.1016/j.procir.2016.06.028

2. Problem definition

The Spar Cap Fitting is a critical part responsible for the load discharge from the sparse to the fuselage. Fitting are used to join the wings together with the fuselage. It can be differentiated into two types:

- Right and left wing are joined together and later attached at the fuselage. In this structure the fitting is loaded only at torsion and transverse force.
- Wings are connected to the fuselage separately. In this manner, the fitting is subjected at bending, torsion moment and transverse force.

In our case the second type is analysed simplifying the torsion moment due to the simplicity of the aircraft in object. This part is a primary structure elements and a failure in this may lead to a catastrophic effect on the airframe.

Taking as example the approach in the load estimation of (4) and (5) a load on the joint can be estimated easily in a preliminary way. This approach has been applied a UAV MALE hybrid designed in Polytechnic of Turin that had similar fittings. This application results with a lower weight and loads.

Figure 1 Plant View of the UAV

As said before the aircraft joint is subjected in this case only at traction and bending moment. These are, obviously, maximum at the root of the spar there the half wing and the fuselage are connected. The load estimation has been carried out as follows.

Starting from the Wing span, 20 meters and to the MTOW, 4018 kg and considering a maximum positive Load Factor, derived to the FAA Normative of 3.8 (in absence of the standard for UAV has been taken the one for normal and commuter airplanes) (6). The design Limit Load can be obtained as follows:

$$Load_{limit} = MTOW * Safety_{Factor} \quad (1)$$

So, a limit load of 15270 Kg has been obtained. To the limit load the structural safety factor of 1.15 (acceptable for well-known materials) has been superimposed obtaining a Ultimate Load of 17560 Kg (or 172092.7 N). Assuming a distribution of the load Wing-Fuselage of 75%-25% as sustained by Jenkinson et al (7) the ultimate load on wing can be obtained as follows:

$$Ultimate_{load} = Structural_{factor} * Load_{limit} * 0.75 * 0.5 \quad (2)$$

A value of 6585 kg (644534 N) has been obtained acting on a single wing.

Considering that there are two spars and that the main one sustain the 55% of the total wing the FEM topology optimization has been carried out only for the main one. in this manner, the joint is subjected to resist at a load of 35530 N distributed according the elliptical distribution of the Lift over the wing span.

To estimate the bending moment the elliptical distribution has been simplified with a resultant force applied to the first third of the wing span as in figure 2.

Figure 2 Lift Artistic Distribution Draft

With the Lift Load estimated as reported before and placed at the first third position of the wing span, using the Moment Transport Rule it is possible to calculate the resulting bending moment at the root. A view of the analyzed considered model is shown in Fig. 3.

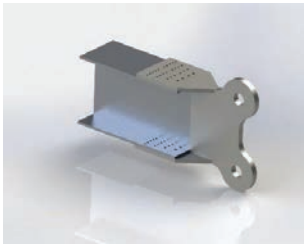

Figure 3 Original Joint View with portion of Spar

3. Analysis and optimization Framework

In (8) the authors proposed the use of topology optimization aimed to components of an UAV to be produced with FDM 3D printing. Hereafter the comparison is focused on the influence that manufacturing process have in the part performance.

The workflow follows the same milestones: first design of the rough model, then optimizing, post processing and re-analysis. To perform this study Hypermesh was used as a pre-processor and Optistruct as solver and optimizer.

To give the maximum freedom to the topological optimization the elements used were all 3-dimensional instead of shell elements.

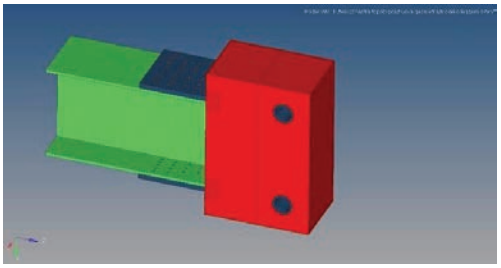

Figure 4 Model Meshing

In Fig 4 is reported a view of the meshed model used. Compared to the original version reported in Fig 3 the spar

end remains the same (in green) while the joint design has changed. The design zone, here reported in red occupies all thee free volume to give to the topological optimization the maximum freedom in the choosing of the best design. Only the holes, in Fig. 4 in blue are non-design space so will not be varied during the optimization. The component presents in three different parts because it has been split in different regions to ease the HEXA meshing process and to have lower dimension on the thin zone and greater on the thicker one.

The spar is meshed as RTRIA based elements growth as tetras (obtained by splitting a QUAD) of uniform dimension of 5mm. In this way, there are at least 4 elements on each thinner side.

Wing joint has two kind of meshing: non-design part is meshed as the spar, TETRA RTRIA of dimension 5mm and the design volume (red in Fig.5) is meshed with HEXA elements of dimension 5 mm with 40 elements on each thin side.

All the components in the optimization run were connected without the use of connecting surface, instead the preference were given to the mesh continuity This choice was taken for the following reason: to have a lighter and faster optimization, considering the incompatibility between the contact surface and the code for the lattice optimization.

The load consists, as previously explained, in a force and a transport moment: both were applied in the cut section of the spar. The constrains were SPC and are applied on the internal nodes of the spar cap; this loads were used through a superposition to set a linear static analysis. In Fig.5 loads are reported in dark purple while SPC in light green.

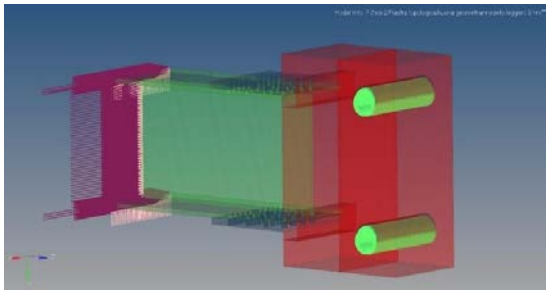

Figure 5 Design and Non-Design parts on the model

The topology optimization was carried out with Optistruct. This tool uses a gradient-based method. Two different optimization were set in parallel:

- A standard topology optimization as done by (9)
- A lattice optimization

Both the optimization run has been done with the same objective and constrains: minimize the compliance with an upper boundary constraint on the mass of the 22% of the global design space. Moreover, another constrain of 600MPa was settled on the design space elements to avoid yielding, and 2 maximum displacements constrain of 2mm for the joint and 5mm for the spar. Only for the classic topology optimization was set the minimum member size and a maximum member size following the suggestion of (10).

The lattice optimization has been a two-phase process. The first phase performs a concept-level topology optimization to optimally partition solid, void, and intermediate space and create the lattice elements. The second phase optimizes the size of each lattice element to determine the final optimized structure. The lattice structure has a cubic shape with a central point connecting to all the vertices, a combination of solid an and b of Fig.7 (11).

4. Additive manufacturing

In this work a comparison between a traditional manufacturing process and additive manufacturing has been proposed to demonstrate the possibilities of mass reduction or stiffening of this technique if applied in a concurrent design process. As sustained by (8) Additive Manufacturing is a promising technique and ready to reach high level of TRL. The most important advantage here reported is the design freedom that allows to construct parts with evolutive shapes that can have better performance respect to the classical obtainable via milling or turning.

4.1. Technology description

The technology chosen for this part among the various available is powder bed technology in its two variants of SLM and EBM. In figure 3 a scheme of Powder Bed Machines is reported.

Figure 6 Powder Bed Machines, courtesy of Fraunhofer IFAM

The main difference from SLM and EMB is the source of power needed to melt the powder in the layer. In the first case is a laser while in the second is a beam of electrons opportunely deflected and focused by a magnetic mirror. Technologically, the first type, SLM is called as a cold process because the bed is not pre-heated before the melting while the second is. This fact allows an increasing of the design freedom due to the compacting of the powder during the pre-heating and a reduction of the residual stresses. More information about the differences and the machine types are available on (3). However, the simulation with EBM technique has been postponed due to the absence of machines with build envelope large enough to contain the entire part.

4.2. Lattice structures

Cellular metals and metallic foams are metals with pores deliberately integrated in their structure; they have combinations of properties that cannot be obtained with dense materials (12) (13). One of the possible applications of cellular materials is the structural usage; the most classic example is their use in sandwich panels. For such structures

the compressive modulus and strength at different relative densities can be estimated by the Gibson Ashby (14) model using the formulae:

$$E/E_0 = C_1 * (\rho/\rho_0)^2 \quad (3)$$

$$\sigma/\sigma_0 = C_2 * (\rho/\rho_0)^{1.5} \quad (4)$$

where E and 6 are respectively the compressive modulus and the strength of the porous material, E_0 and 6_0 are respectively the compressive modulus and the strength of the dense material, C_1 and C_2 are specific constant.

Unlike traditional manufacturing methods, additive manufacturing can produce parts with complex geometric structures without significant increases in fabrication time. One application of the additive manufacturing technologies is the fabrication of customized lattice-skin structures such as periodic lattice pattern that cannot be manufactured in any other technology (15).

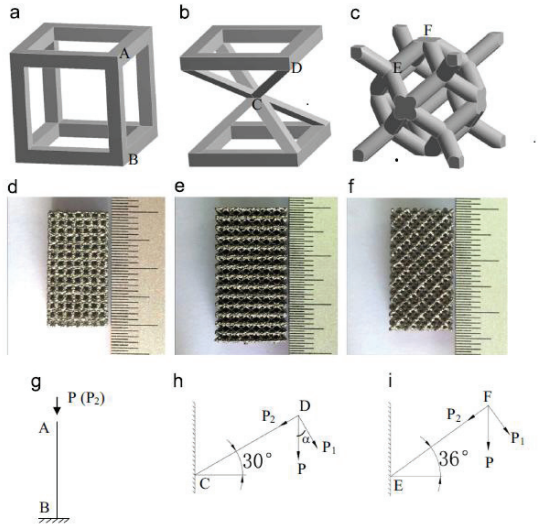

Figure 7 Lattice structures Fabricated with EBM (11)

In this work one optimization has been conducted to evaluate, although in a preliminary way, its performance and possible applications to structural parts of Unmanned Aircraft.

5. Milling

The original part was designed to be manufactured via milling process and weights 31.473 kg. Milling is a machining workflow that uses rotary cutters to remove material from a workpiece by advancing in a predefined direction and angles. This process is the most common used in industrial production for what concerning metal forming of aerospace structures (16).

The main machining activities performed on this component are milling, drilling and (in special cases) welding phase. Raw plates are of design thickness and are pre-formed by plasma cutting to have a raw design profile with meanly 5 mm of machining allowance. All machine tools have mean workpiece constrains and automatic toolpath management systems, but in the work time calculation the positioning of workpiece and toolpath changes are neglected to improve accuracy since additive manufacturing process does not present equivalence ones. Although it is possible estimate an additional time of 30% to the total production time to have a realistic evaluation of these neglected activities. Instead of the welding phase of the three-plate element after drilling and milling, is properly performed and simulated by reference table 1 according to (17) welding certification process. The welding times is estimated considering the following process parameter:

- Coupling geometry for two elements to connect;
- Element Thickness and material properties;
- Welding Method parameters;
- Linear welding distance expressed in millimetres;

The mean welding velocity for all considered materials is estimated in 100mm/min using GMAW as welding method using 300 Amperes for current electrodes (18). Therefore, the welding time process estimated on 606.28 mm of linear welding path is 3500 seconds to produce a complete assembly. The welding process needs further verifications to avoid defects affecting the fatigue resistance. These NDT (Non-destructive Tests) verifications times are neglecting in the time production to improve accuracy comparison since additive manufacturing presents equivalent ones.

The drilling and milling phase for the proposed CAD part geometry, illustrated on Fig.3, are overall calculated by Unigraphics Nx CAM module ver. 7 using default 3 Axis machine parameters inside the software module. The production times of each assembly part is illustrated always on table 1.

Part Name	Drilling Phase [s]	Milling Phase [s]	Material	Total [s]
SPAR_1	678	783	AISI4340	1461
SPAR_2	120	1445	AISI4340	1565
SPAR_3	678	783	AISI4340	1461
ASSEMBLY	1476	3011	AISI4340	4487

Table 1 production times for each plane milling, and drilling phase

Therefore, the whole production time for assembly workpiece is 4487 seconds for AISI4340. The assembly after both additive manufacturing or usual production process needs further processes of peeing and aluminizing to respectively improve fatigue and oxidation stability performances.

6. Results

The results presented here are a comparison on different aspects (manufacturing time, structural resistance, etc.) for a critical component of a UAV structure. Firstly, will be presented the topological optimization for a solid part to be constructed with AM showing a comparison with the original made by milling. The second part of this section will focus on the lattice structure and its criticality. Both the solution has been simulated in a EOS M400 DMLS to evaluate the time requested to manufacture the part with a result of 80 hours for the solid solution and 95 hours for the lattice one. the simulation in EBM machines had not been possible due to the absence, at the moment, of machine large enough to construct the part in one single piece (19).

6.1. Solid part

The optimization was carried on following the process reported in section 3. In Fig. 8a it is possible to see that the optimized distribution of mass goes from the top of the spar to the holes directly. The optimization also suggests a cross structure to stiffen the joint. Taking the results from Optistruct the redesign process was done using the Nurbify Tool. In this manner, a Poly-Nurbs solid can be fitted to model the evolutive shape obtained from the topological optimization. It has been chosen this approach because of the difficulties of classical CAD features on modelling such shapes. In Fig 8b is reported an artistic view the re-designed structure.

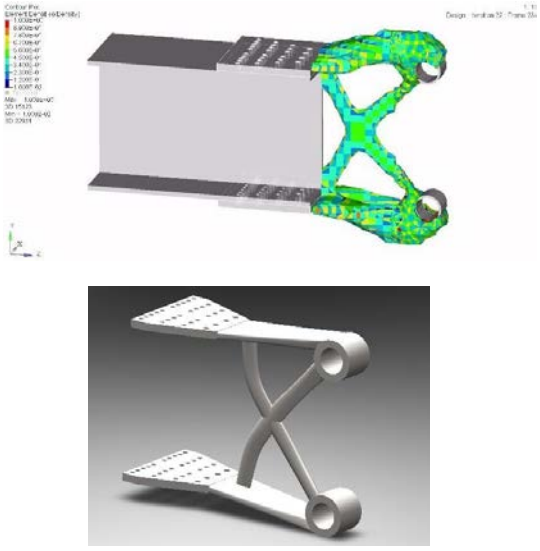

Figure 8 a- Contour density plot of the optimization result; b-Redesign, artistic view

Hereafter are reported the results of the analysis done on the joint after the redesign to verify that the simplification of the nurbify phase had not caused criticalities. The re-designed components have a final mass of 15.715 kg. The pictures show that the maximum stresses are near to 250 MPa, well below the 600 MPa of yielding imposed as constraint. The maximum displacement occurs at the top of the connection between the joint and the spar and it is of 0.346 mm.

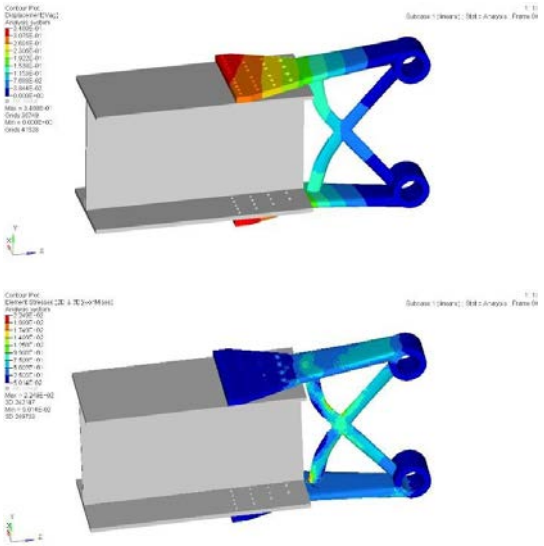

Figure 9 a-Displacement on the re-designed joint; b-Stresses (Von Mises) on the re-designed joint

6.2. Lattice structured Part

As described before in section 3 the lattice optimization was a two-step process; the first is a topological optimization with particular constraint and its results are plotted in Fig 10a. It is similar to those shown in Fig. 8a, except for the stiffening rods that have been removed from the Optimizer due to the embedded manufacturing constraint. After the first step, there is a size and shape optimization where diameter of the dipstick and the cell size are varied to minimize the compliance while keeping the mass below the boundary constraint of the 22%.

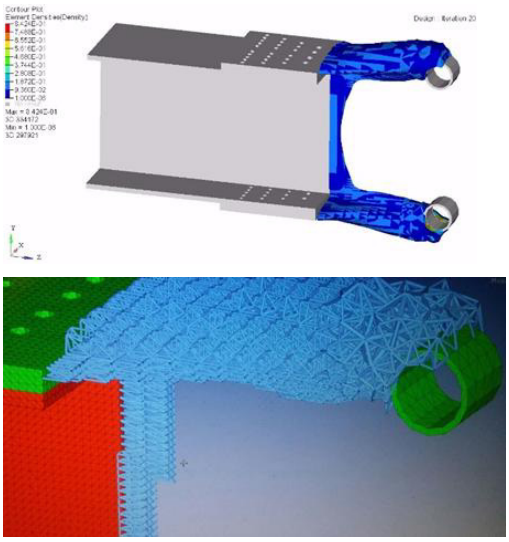

Figure 10 a-Contour density plot of the optimization result; b-View of the cellular structure

After this optimization, as before, a second run of check on the proposed solution has been done and the results are reported in Fig. 11. The components have reached a final mass of 14.027 kg. The maximum displacement in the joint has grown at 1.83 mm because of the light and flexible cells structure while the maximum shear stress, measured in the beam is equal to 203 MPa. However, for this results further analysis are requested to evaluate the effective behaviour of the lattice under loading and at fatigue. This analysis must be intended as an explorative solution of feasibility.

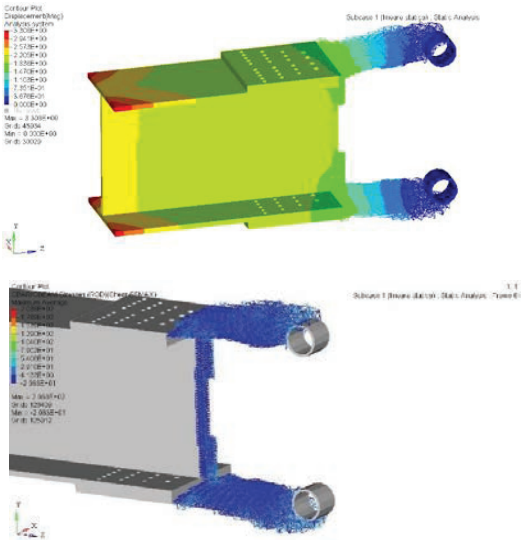

Figure 11 a- Displacement on the system joint-spar with the lattice solution; b-Stresses (Von Mises) on the re-designed joint with the lattice solution

7. Conclusions

In this work an existing part has been reviewed changing the manufacturing technology to evaluate if there was some sort of convenience both from structural and manufactural point of view. It has been shown that milling process requires 1.24 hours to manufacture the part (drilling, milling and welding) without considering of the controls and the set-up time. Additive manufacturing requires at least 80 hours to complete the building. So, for large series there is not now advantage in terms of manufacturing efficiency due to the slowness of the AM process.

The advantage instead is in terms of performance: with the design freedom of the AM is possible to build in a single part geometries impossible to build with other manufacturing technique (for example lattice structures or evolutive shapes). The mass reduction achievable of the 50% (from 31.473 kg to 15.715 kg or 14.027 kg) in aeronautics is of interest because it can reduce the global mass and so improve the flight endurance of the mission when applied at the whole primary structure.

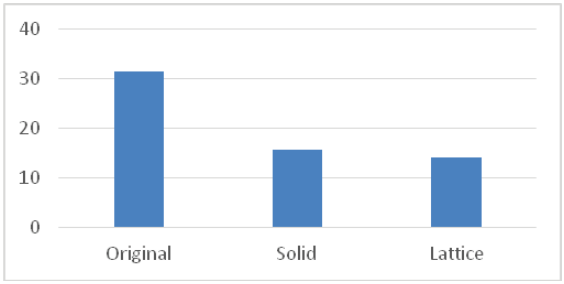

Figure 12 Joint Masses

Moreover, small or extra small series such as Fixed Wing UAV, for patrol or reconnaissance role, can tolerate the increase of cost due to the minimum number of parts to be constructed.

For what concerns the Lattice structure, however, this analysis must be intended just as a preliminary and explorative one. Further improvements will be required to understand the effective behaviour of such structures.

8. Acknowledgements

The authors thank Massimo De Salvo, Leader Technologist at Data Network Consulting S.r.l, for the important advices that greatly improved the manuscript. We would also like to show our gratitude to Altair Engineering, especially to Giulio Turinetti for the constant support.

References

1. **Austin, Reg.** *Unmanned Aircraft Systems.* 2010.
2. **ACARE.** *Creating innovative air transport technoogies for Europe.* s.l. : European Union, 2013.
3. **Wohlers.** *Wohlers Report.* 2015.
4. *Design and Analysis of Wing fuselage attachment bracket for fighter.* **Shashikumar.C, Nagesh.N, Ganesh.** 2016, International Journal of Engineering Research and General Science.
5. *Stress Analysis and Fatigue Life Prediction of Wing-Fuselage Lug Joint Attachment Bracket of a Transport Aircraft.* **Sriranga B.k, Kumar .R.** 2014, IJRET: International Journal of Research in Engineering and Technology.
6. *Part 23 Airworthiness standards: normal, utility acrobatic and commuter category airplanes.* **FAA.**
7. **Jenkinson, Lloyd R.** *Aircraft Design.* Oxford : Butterworth Heinemann.
8. *Additive Manufacturing Offers New Opportunities in UAV Research.* **Carlo Ferro, Roberto Grassi, Carlo Seclì, Paolo Maggiore.** s.l. : Elsevier, 2016, Vol. Vol. 41.
9. *Three-dimensional Topologies of Compliant Flapping Mechanism.* **Stanford, Bret.** 4, s.l. : ASCE Journal of Aerospace Engineering, 2014, Vol. 27.
10. **Matthias, Goelke.** *Pratical Aspects of structural Optimization.* 2014.
11. *The influence of cell morphology on the compressive fatigue behavior of Ti6Al4V meshes fabricated by electron*

beam melting. **S.J.Li, W.T.Hou Y.L.Hao R.Yang R.D.K.Misra S. Zhaoa.** s.l. : Journal of th mechanical behavior of biomedical materials, 2016.
12. *Porous Metals and Metallic Foams: Current Status and Recent Developments.* **Banhart, David C. Dunand Louis-Philippe Lefebvre John.** 9, s.l. : Advanced Engineering Materials, 2008, Vol. 10.
13. **Lorna J Gibson, Michael Ashby.** *Cellular Solids.* .
14. **Ashby, Lorna J. Gibson and Michael F.** *Cellular Solids: Structure and Properties.* s.l. : Cambridge Univ. Press., 1997.
15. *Bidirectional Evolutionary Structural Optimization (BESO) based design method for lattice structure to be fabricated by additive manufacturing.* **Kurtz, Yaoyao Fiona Zhao Yunlong Tang Aidan.** s.l. : Computer Aided Design, 2015, Vol. 69.
16. **Todd, Robert H., Allen, Dell K. and Alting, Leo.** *Manufacturing processes reference guide.* New York : New York: Industrial Press, 1994. ISBN 978-0-8311-3049-7.
17. **Society, American Welding.** *Welding Handbook, Welding Processes, Part 1.* Miami : s.n., 2004. ISBN 0-87171-729-8.
18. *Study of welding velocity and pulse frequency on microstructure and mechanical properties of pulsed gas metal arc welded high strength low alloy steel* . **M. Mirzaei, R. Arabi Jeshvaghani, A. Yazdi.** s.l. : Materials & Design, 2013, Vol. 51.
19. **Ab, Arcam.** http://www.arcam.com. [Online]